SUPPORTING INFORMATION

Determination of Ligand-Field Parameters and their Related Errors. Axial (Δ/λ) and rhombic (V/λ) ligand-field terms are determined from the experimental g values according to the following equations:

$$\frac{V}{\lambda} = \frac{E_{yz}}{\lambda} - \frac{E_{xz}}{\lambda} = \frac{g_{xx}}{g_{zz}+g_{yy}} + \frac{g_{yy}}{g_{zz}-g_{xx}} \quad (1)$$

$$\frac{\Delta}{\lambda} = \frac{E_{yz}}{\lambda} - \frac{E_{xy}}{\lambda} - \frac{V}{2\lambda} = \frac{g_{xx}}{g_{zz}+g_{yy}} + \frac{g_{zz}}{g_{yy}-g_{xx}} - \frac{V}{2\lambda} \quad (2)$$

Use of these equations requires that the normalization condition holds:

$$g_{xx}^2 + g_{yy}^2 + g_{zz}^2 + g_y g_z - g_x g_z - g_x g_y - 4(g_{zz} + g_{yy} - g_{xx}) = 0 \quad (3)$$

The orbital coefficients (a, b, c) are related to g-tensor values by the following equations (note: $g_{zz} = g_{max}$; $g_{yy} = g_{mid}$; $g_{xx} = g_{min}$):

$$a = (g_{max} + g_{mid}) / D \quad (4a)$$

$$b = (g_{max} - g_{min}) / D \quad (4b)$$

$$c = (g_{mid} - g_{min}) / D \quad (4c)$$

Where $D = \sqrt{8} \times (g_{zz} + g_{yy} - g_{xx})$ (5)

and

$$\Sigma (a)^2 + (b)^2 + (c)^2 = 1.00 \pm 0.01 \quad (6)$$

The ligand-field terms can be described in terms of orbital coefficients by:

$$\frac{V}{\lambda} = \frac{a+c}{2b} - \frac{b+c}{2a} \quad (7)$$

and

$$\Delta = B - V/2\lambda \quad (8)$$

where

$$B = \frac{a+b}{2c} - \frac{b+c}{2a} \quad (9)$$

In addition, the quantity "A" is defined (for use below, see Figure S1) as:

$$A = V/\lambda. \qquad (10)$$

From CW-EPR measurements the signs (+ / −) of the *g*-tensor components cannot be determined; they can be either positive or negative. Calculation of the relevant ligand-field parameters (V, Δ) starting from a combination of *g*-tensor values together with the coefficients (a, b, c) and related values defined above (A, B and D) can be obtained by solving equations 1-10 with the help of the freeware program developed by N. V. Shokhirev and A. F Walker (2000), University of Arizona, Department of Chemistry (download at http://www.shokhirev.com/nikolai/projects/gxyz/gxyz10.html). An example of the program output obtained for a limited combination of different signs for the *g*-tensor components in *Ht c*-552 is given in the figure below (Figure S1).

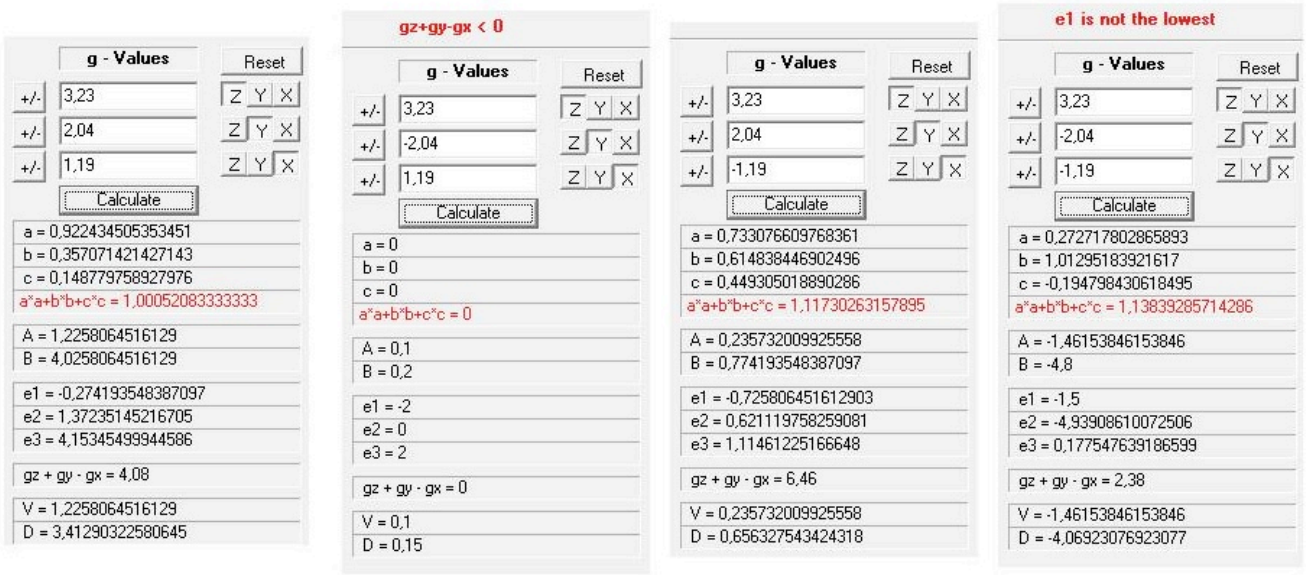

Figure S1. Orbital coefficients (a, b, c) and ligand-field parameters (V, Δ) calculated for the experimentally measured *g*-values of *Ht c*-552 where it has been assumed that the signs of the *g*-tensor components could be positive or negative (+ / −).

In the calculation shown in Figure S1, it is important to emphasize that not all combinations of *g*-tensor values are possible. One additional constraint is required, that the sum $g_{zz} + g_{yy} - g_{xx} > 0$, in order to avoid the possibility that solutions for equation (5) include imaginary values for D (e.g D = $\sqrt{8} \times (-$ number)). Huynh and coworkers[1] demonstrated that the product of the three principal *g*-tensor values was positive in the case of cytochrome c_2 from *Rhodospirillum rubrum* through Mössbauer spectroscopy. We have also determined the same positive *g*-tensor product in the cytochrome *Nitrosomonas europaea* cytochrome *c*-552, which exhibits a large g_{max} value, through Mössbauer spectroscopy.[2] Thus, we assumed in the analyses of EPR data that the signs of the *g*-tensor components are all positive also in *Ht c*-552 and *Pa c*-551 variants. In order to determine the errors in ligand-field parameters, EPR spectra simulations are necessary. The following method can be employed when not all *g*-values are detected clearly in the spectrum; two defined *g*-tensor values are initially chosen from the experimental EPR spectrum together with their errors (determined from the uncertainties in the magnetic field observed in the actual spectrum, *vide infra*), and the third value is extracted using equation (3), which must fulfil equation (6), $\Sigma\ (a)^2 + (b)^2 + (c)^2 = 1.00 \pm 0.01$. By keeping a constant line-width tensor in the spin-Hamiltonian parameters within the simulated series of resonances, each simulated spectrum is then compared with the experimental, and the error in ligand-field terms is derived as shown in Tables S1-S5. Note that the uncertainties in the magnetic field and hence in the observed *g*-values come primarily as consequence of the experimental EPR settings employed. Several factors can alter the resonance line. Once we exclude phenomena such as saturation of the resonance line due to the use of very high microwave power (used for example to improve the signal-to-noise ratio) and fast passage effects due to not well calibrated (e.g. too short) magnetic field sweep-times, the spectrum resolution (and hence accuracy of the *g*-value) is strongly influenced by: (total field sweep width) / (number of magnetic field points in resonance). In our settings we employed a 7000-Gauss sweep width over 1024 resonance points. Thus, the spacing between adjacent

resonances or the maximum of the resonance line can be resolved down to ~ 6.8 Gauss (7000 Gauss/1024 = 6.836 Gauss). This uncertainty must be taken into account when we decide the dimension of the modulation amplitude to be employed within EPR data acquisition. In our experiments we employed modulation amplitudes of 7 Gauss, hence slightly larger than the expected field resolution. Under such experimental settings, for *g* values falling around 3.2, if the EPR resonance signature exhibits a well-resolved Gaussian line shape such as the envelopes observed in our spectra, an error of $\Delta g = \pm 0.01$ in g_{max} is estimated. However, the error in *g*-value assessed from the experimentally observed EPR resonance envelope can be doubled or even more for broad and/or weak resonance lines (e.g in the high-field region where $\Delta g_{min} = \pm 0.02$).

Table S1: Error distribution in the *g*-tensor and calculated ligand-field values for *Ht c*-552

g_{max}	g_{mid}	g_{min}	D	*a*	*b*	*c*	*V*	B	Δ	$\Sigma(a,b,c)^2$	*V*/Δ
3.23	2.04	1.19	5.71	0.922	0.357	0.149	1.23	4.03	3.41	1.00	0.359
3.22	2.03	1.21	5.69	0.923	0.354	0.144	1.24	4.16	3.54	1.00	0.351
3.24	2.05	1.17	5.74	0.921	0.361	0.153	1.21	3.90	3.30	1.00	0.367
3.22	2.05	1.21	5.70	0.925	0.353	0.147	1.25	4.06	3.44	1.00	0.363
3.24	2.03	1.17	5.73	0.920	0.361	0.150	1.20	3.99	3.39	1.00	0.355
3.22	2.03	1.17	5.71	0.919	0.359	0.151	1.21	3.97	3.36	1.00	0.361
3.23	2.04	1.21	5.70	0.925	0.354	0.146	1.24	4.12	3.50	1.00	0.354
3.24	2.05	1.21	5.71	0.926	0.355	0.147	1.24	4.09	3.47	1.01	0.357
3.23	2.05	1.19	5.72	0.923	0.357	0.150	1.23	3.98	3.37	1.00	0.366
3.24	2.03	1.19	5.71	0.922	0.359	0.147	1.22	4.08	3.47	1.00	0.350

Table S2: Error distribution in the *g*-tensor and calculated ligand-field values for *Ht*K22M

g_{max}	g_{mid}	g_{min}	D	*a*	*b*	*c*	*V*	B	Δ	$\Sigma(a,b,c)^2$	*V*/Δ
3.23	2.08	1.19	5.74	0.925	0.355	0.155	1.24	3.85	3.23	1.01	0.385
3.22	2.07	1.17	5.74	0.921	0.357	0.157	1.23	3.80	3.18	1.00	0.387
3.22	2.07	1.21	5.71	0.926	0.352	0.151	1.26	3.97	3.34	1.00	0.376
3.24	2.09	1.17	5.77	0.924	0.359	0.159	1.23	3.74	3.13	1.01	0.393
3.24	2.09	1.21	5.74	0.928	0.354	0.153	1.26	3.91	3.28	1.01	0.383
3.23	2.09	1.20	5.74	0.927	0.354	0.155	1.26	3.85	3.23	1.01	0.389
3.23	2.09	1.21	5.73	0.928	0.352	0.153	1.26	3.90	3.27	1.01	0.386
3.22	2.09	1.21	5.73	0.927	0.351	0.154	1.27	3.89	3.25	1.01	0.390
3.22	2.08	1.19	5.73	0.924	0.354	0.155	1.25	3.84	3.22	1.00	0.388
3.24	2.07	1.21	5.73	0.927	0.354	0.150	1.25	4.00	3.37	1.01	0.370

Table S3: Error distribution in the *g*-tensor and calculated ligand-field values for *Ht*M13V

g_{max}	g_{mid}	g_{min}	D	*a*	*b*	*c*	*V*	B	Δ	$\Sigma(a,b,c)^2$	*V*/Δ
3.19	2.09	1.17	5.73	0.921	0.352	0.160	1.26	3.69	3.06	1.00	0.410
3.18	2.08	1.19	5.71	0.922	0.349	0.156	1.27	3.80	3.16	1.00	0.402
3.2	2.10	1.15	5.76	0.920	0.356	0.165	1.24	3.59	2.96	1.00	0.419
3.19	2.08	1.18	5.72	0.921	0.351	0.157	1.26	3.77	3.14	1.00	0.401
3.18	2.10	1.17	5.73	0.921	0.351	0.162	1.27	3.64	3.01	1.00	0.421
3.18	2.09	1.16	5.73	0.919	0.352	0.162	1.25	3.64	3.01	1.00	0.417
3.19	2.08	1.19	5.71	0.922	0.350	0.156	1.27	3.81	3.18	1.00	0.398
3.19	2.10	1.15	5.76	0.919	0.354	0.165	1.25	3.58	2.95	1.00	0.422
3.19	2.09	1.17	5.73	0.921	0.352	0.160	1.26	3.69	3.06	1.00	0.410
3.18	2.08	1.19	5.71	0.922	0.349	0.156	1.27	3.80	3.16	1.00	0.402

Table S4: Error distribution in the *g*-tensor and calculated ligand-field values for *Ht*M13V/K22M

g_{max}	g_{mid}	g_{min}	D	*a*	*b*	*c*	*V*	B	Δ	$\Sigma(a,b,c)^2$	V/ Δ
3.17	2.11	1.17	5.73	0.921	0.349	0.164	1.28	3.59	2.96	1.00	0.432
3.16	2.12	1.18	5.73	0.922	0.346	0.164	1.29	3.59	2.94	1.00	0.440
3.17	2.10	1.17	5.73	0.920	0.349	0.162	1.27	3.63	2.99	1.00	0.425
3.18	2.11	1.17	5.74	0.921	0.350	0.164	1.27	3.60	2.97	1.00	0.428
3.16	2.10	1.16	5.73	0.918	0.349	0.164	1.27	3.58	2.95	0.99	0.431
3.16	2.12	1.16	5.74	0.920	0.348	0.167	1.28	3.51	2.87	1.00	0.446
3.17	2.10	1.16	5.73	0.919	0.351	0.164	1.26	3.59	2.96	0.99	0.427
3.18	2.12	1.16	5.76	0.921	0.351	0.167	1.27	3.53	2.90	1.00	0.438

Table S5: Error distribution in the *g*-tensor and calculated ligand-field values for *Pa*F7A

g_{max}	g_{mid}	g_{min}	D	*a*	*b*	*c*	*V*	B	Δ	$\Sigma(a,b,c)^2$	*V*/Δ
3.15	2.09	1.15	5.72	0.916	0.350	0.164	1.26	3.57	2.94	0.99	0.430
3.14	2.10	1.15	5.72	0.916	0.348	0.166	1.27	3.52	2.89	0.99	0.441
3.14	2.09	1.16	5.71	0.917	0.347	0.163	1.28	3.60	2.96	0.99	0.432
3.16	2.09	1.16	5.72	0.918	0.350	0.163	1.27	3.62	2.99	0.99	0.424
3.16	2.08	1.14	5.73	0.915	0.353	0.164	1.25	3.58	2.96	0.99	0.422
3.15	2.10	1.14	5.73	0.916	0.351	0.167	1.26	3.50	2.87	0.99	0.440
3.15	2.08	1.14	5.72	0.914	0.351	0.164	1.25	3.57	2.94	0.99	0.426
3.14	2.10	1.16	5.71	0.917	0.347	0.165	1.28	3.56	2.92	0.99	0.439
3.16	2.10	1.15	5.73	0.917	0.351	0.166	1.26	3.54	2.91	0.99	0.434
3.15	2.09	1.15	5.72	0.916	0.350	0.164	1.26	3.57	2.94	0.99	0.430

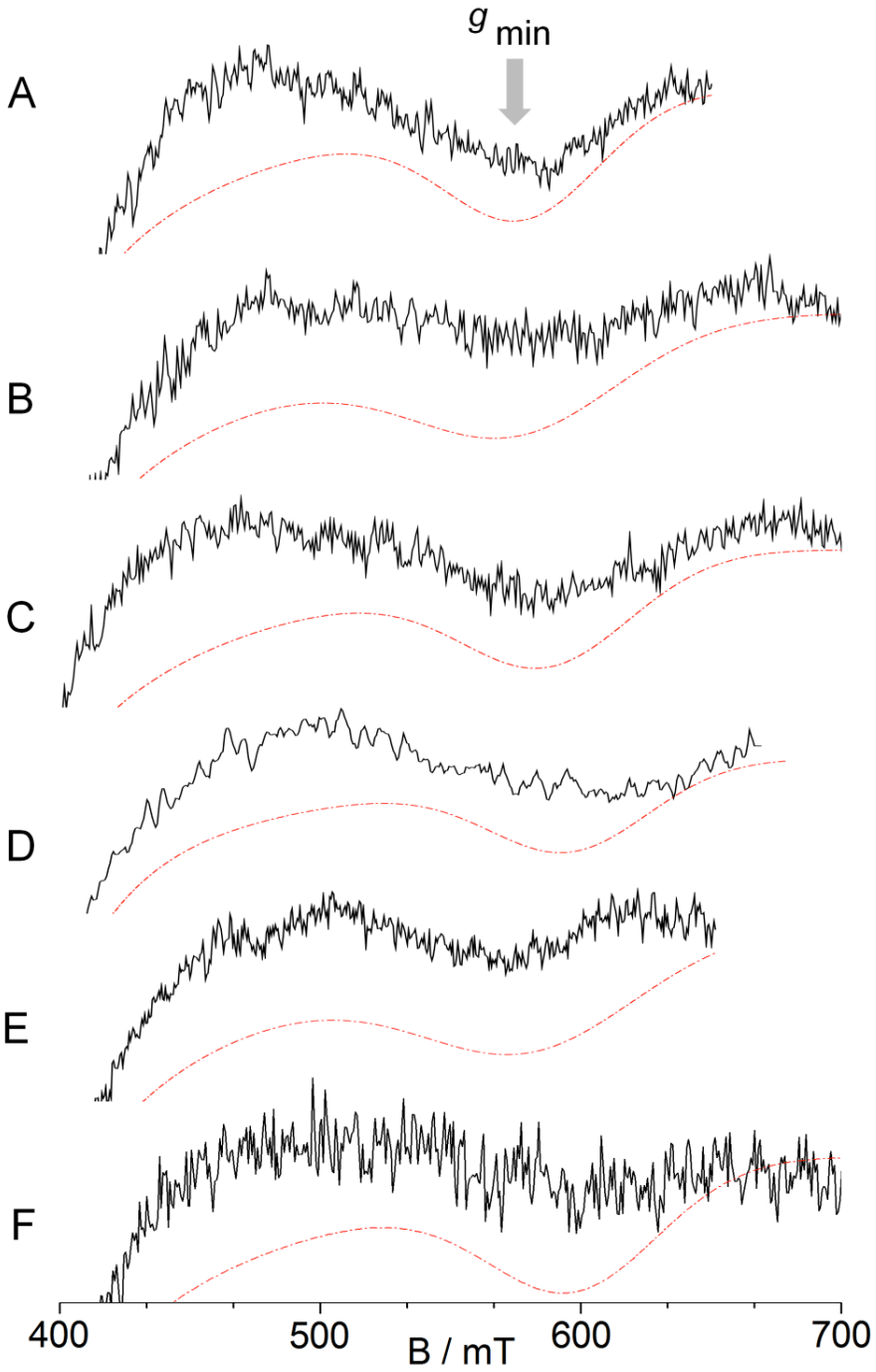

Figure S2. X-band (9.663(8) GHz) EPR spectra of *Ht c*-552 and *Pa c*-551 and selected variants in the high-field region (around g_{min}): (A) *Ht c*-552, (B) *Ht*-K22M, (C) *Ht*-M13V, (D) *Ht*-MI3V/K22M, (E) *Pa c*-551, (F) *Pa* F7A. Samples were 200-300 µM protein in 50 mM HEPES. pH 7.5. Measurements were performed at a temperature of 9.0 ± 1.0 K. The dashed red lines represent simulated EPR envelopes. The best set of *g*-tensor values is given in Table 1.

References:

1. Huynh, B. H.; Emptage, M. H.; Münck, E. *Biochim Biophys Acta* **1978**, *534*, 295–306.
2. Zoppellaro, G.; Teschner, T.; Harbitz, E.; Schu¨nemann, V.; Karlsen, S.; Arciero, D. M.; Ciurli, S.; Trautwein, A. X.; Hooper, A. B.; Andersson, K. K. *Chem Phys Chem* **2006**, *7*, 1258–1267.